ACS Energy LETTERS

http://pubs.acs.org/journal/aelccp

Direct Optical Lithography of Colloidal InP-Based Quantum Dots with Ligand Pair Treatment

Jaehwan Lee, Jaeyeong Ha, Hyungdoh Lee, Hyunjin Cho, Doh C. Lee, Dmitri V. Talapin,* and Himchan Cho*

Cite This: *ACS Energy Lett.* 2023, 8, 4210−4217

Read Online

ACCESS | Metrics & More | Article Recommendations | Supporting Information

ABSTRACT: Direct optical lithography presents a promising patterning method for colloidal quantum dots (QDs). However, additional care needs to be taken to prevent deterioration of the optical properties of QDs upon patterning, especially for InP-based QDs. This study proposes an efficient method for high-resolution patterning of InP-based QDs using a photoacid generator while preserving their optical properties. Specifically, our solid-state ligand exchange strategy, replacing chloride ligands with long-chain amine/carboxylate pair ligands, successfully recovered the photoluminescence quantum yield (PLQY) of the patterned InP-based QD films to ∼67% of the original PLQY. Upon examination of the origins of the PLQY reduction during patterning, we concluded that the formation of deep traps caused by the exchanged chloride ligands was the primary cause. Finally, we fabricated high-resolution (feature size: 1 μm), multicolored patterns of InP-based QDs, thereby demonstrating the potential of the proposed patterning method for next-generation high-resolution displays and optoelectronic devices.

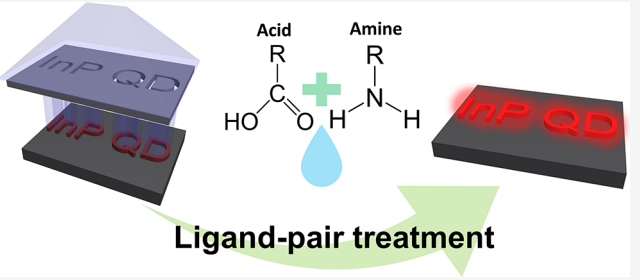

Colloidal quantum dots (QDs) constitute a promising class of next-generation optoelectronic materials that exhibit large absorption coefficients, high photoluminescence quantum yields (PLQY), and excellent color purity.[1−3] Based on the extensive research conducted on the synthesis methods and characteristics of InP QDs, they have recently been adopted as color conversion layers for commercial TVs owing to their low toxicity.[4−8] To implement QDs in next-generation displays such as augmented reality glasses, the QD layer must be uniformly patterned into red, green, and blue (RGB) subpixels at a scale of a few micrometers or less.[9]

Direct optical lithography of functional inorganic nanomaterials (DOLFIN) is an emerging patterning technique that uses a photosensitive moiety in the nanomaterial ink to create patterns instead of using prepatterns of conventional photoresist.[10] DOLFIN yields highly uniform high-resolution QD patterns without involving complicated steps of conventional photolithography (Figure S1).[10] The variations of DOLFIN can be classified according to the patterning mechanism that utilizes a (1) photoacid generator (PAG),[11,12] (2) ligand cleavage,[13,14] (3) ligand cross-linking,[15−19] and (4) photobase generator.[20] In the case of PAG-based DOLFIN, a ligand exchange process is not required before patterning, which is advantageous for reducing surface defects and preventing QD aggregation that may occur with the exchange process. The variations in solubility of the light-exposed region are enabled by a small amount of PAG additive (1−2 wt %),[11] which is beneficial for both photoluminescence (PL) down-conversion and electroluminescence (EL) applications. Recently, Fu et al. employed PAG-based direct optical lithography to fabricate patterned high-efficiency CdSe-based QD LEDs.[12]

However, even a small amount of PAG can cause significant variations in the PLQY of the QDs. In our previous study,[11] we reported that an addition of 2 wt % PAG can reduce the PLQY of CdSe-based core/shell QDs by ∼30%. Although recent studies have attempted to address this issue,[10−12,21,22] it has not been completely overcome. In particular, the aforementioned issue is observed to be more critical in the case of InP-based QDs.[23] Thus, to adopt direct optical lithography in InP

Received: May 24, 2023
Accepted: September 5, 2023
Published: September 25, 2023

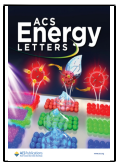

Downloaded via UNIV OF CHICAGO on December 11, 2023 at 19:13:43 (UTC).
See https://pubs.acs.org/sharingguidelines for options on how to legitimately share published articles.

ACS Publications

© 2023 American Chemical Society

https://doi.org/10.1021/acsenergylett.3c01019
ACS Energy Lett. 2023, 8, 4210−4217

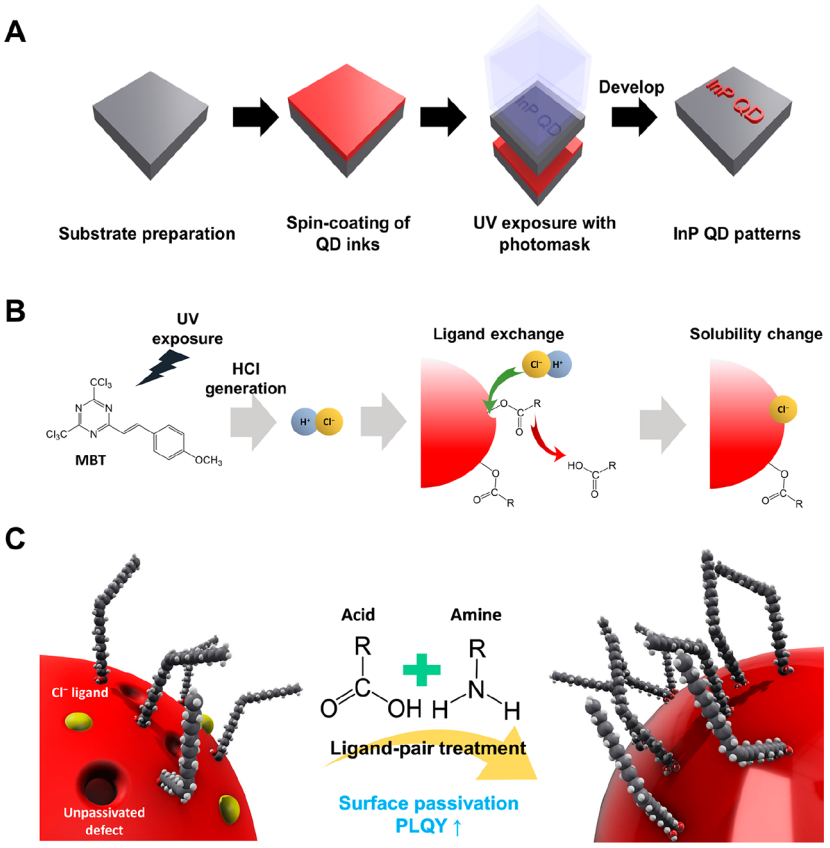

Figure 1. (A–C) Schematics of (A) direct optical lithography process, (B) *in situ* ligand exchange, and (C) a LPT strategy for surface repassivation.

QD-based optoelectronics and displays, the root cause of the PLQY reduction must be revealed with an in-depth analysis of the variations in the luminescence characteristics of InP-based QDs, and accordingly, an advanced patterning strategy should be devised to effectively mitigate the PLQY reduction caused by the patterning process.

This study investigates the reduction in the PLQY of InP/Zn(Se,S) core/shell QDs during PAG-based direct optical lithography and proposes an effective strategy that can recover degraded PLQY, referred to as ligand pair treatment (LPT). The surface environment of the QDs was examined by using various spectroscopic methods, including X-ray photoelectron spectroscopy (XPS), time-resolved photoluminescence (TR-PL), Fourier-transform infrared spectroscopy (FTIR), and transmission electron microscopy (TEM), and the relationship between such surface environment and PLQY was revealed. Based on these analyses, we developed a LPT strategy that can passivate the QD surface with long-chain organic ligands to restore the PLQY of QD patterns. Furthermore, we fabricated high-resolution RGB patterns of InP-based QDs with high uniformity and low line edge roughness (LER), achieving feature sizes as small as 1 μm.

The schematic of the direct optical lithography process is illustrated in Figure 1A, and the InP-based core/shell QDs used herein exhibited PL emission spectra centered at 628 (red) and 519 nm (green) (Figure S2).

Compared to the photophysical properties (e.g., PLQY and emission spectrum) of CdSe-based QDs, those of InP-based QDs are more sensitive to the surface environment (e.g., surface atoms, defects, and ligands).[22−24] Generally, direct optical lithography methods induce chemical alterations at the QD surface upon patterning processes, such as ligand detachment/decomposition[13,14,25−28] and *in situ* ligand exchange.[10,11] These chemical alterations at the QD surface are essential for inducing the solubility variations that cause the formation of QD patterns; however, the photophysical properties of the surface-environment-sensitive InP-based QDs would inevitably degrade upon these variations. Furthermore, due to the high oxophilicity of InP QDs, oxidation of the InP core surface may occur during the patterning process, which involves exposure to high-energy light, acid, oxygen, and moisture. This oxidation process can also lead to a decrease in PLQY. To mitigate the reduction of the photophysical properties of QDs during patterning, we should minimize the ultraviolet (UV) light dose required for patterning and the surface degradation of QDs caused by PAG during the ink formulation and patterning processes. According to our previous study,[11] 2-(4-methoxystyryl)-4,6-bis(trichloromethyl)-1,3,5-triazine (MBT, Figure S3) allows a relatively low UV dose and enables a smaller PLQY reduction than other types of PAGs during the patterning process. By optimizing the ink composition and UV dose, we were able to increase the pattern resolution to the micrometer scale without any background residue and thickness alteration (Figures S4 and S5).

However, even with a minimized UV dose and MBT amount, the final patterns of InP-based QDs manifested a larger reduction in PLQY than CdSe-based QDs. We hypothesize that the reduction in PLQY of InP-based QDs can be attributed to the (1) generation of deep trap states by

https://doi.org/10.1021/acsenergylett.3c01019
ACS Energy Lett. 2023, 8, 4210−4217

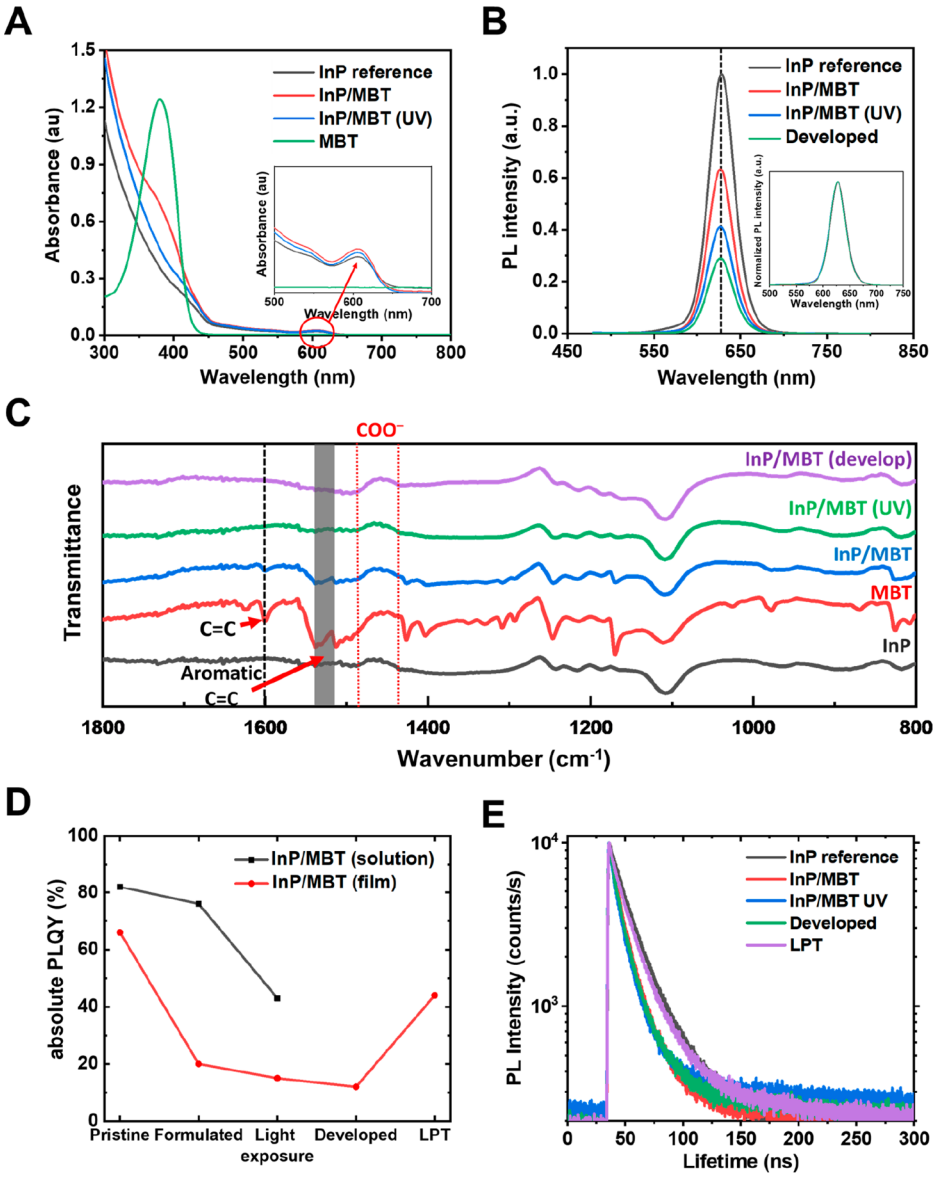

Figure 2. (A) Absorption spectra of InP/Zn(Se,S) core/shell QD (hereafter denoted as "InP" or "InP QD") dispersions. (B) PL spectra of InP QD films at each patterning step. (C) FTIR spectra of InP QD, MBT, InP/MBT, UV-exposed InP/MBT, and developed (patterned) InP QD films. The black dashed line and gray rectangular region denote the MBT characteristic portion, and the red dashed line represents that of carboxylate. (D) Absolute PLQY (dispersion and film, excitation wavelength: 380 nm) and (E) PL lifetime curves (film) of InP QDs at each patterning step and LPT.

photogenerated HCl, (2) oxidation of the QD core during the patterning process, and (3) the presence of residual MBT in the patterned QD films. Exposing QD/MBT films to UV irradiation leads to *in situ* ligand exchange, in which a small portion of long-chain carboxylate ligands is replaced by chloride ligands (Figure 1B). The exchanged chloride ligands may create deep trap states, leading to a decrease in PLQY.[23,29] Additionally, the photogenerated protons can etch the surface of the shell, creating surface defects such as unpassivated sulfur sites that can further contribute to the formation of deep traps.[23] However, as the *in situ* ligand exchange process is a mandatory step for inducing solubility variations, we devised a solid-state ligand exchange strategy, referred to as LPT, to respassivate the unpassivated or chloride ligand-exchanged regions of the patterned QDs with long-chain organic ligands (Figure 1C). In addition to the formation of deep trap states, the PLQY may reduce because of additional factors such as core oxidation or residual MBT after patterning process. Note that the presence of MBT after development can negatively impact the PL characteristics of QD patterns because any remaining MBT can absorb excitation light and decompose, generating protons that could further etch the QD surface.

To discern the root cause of the PLQY reduction among the above possible origins, we performed a comprehensive series of measurements, such as UV/visible spectroscopy (UV/vis), steady-state PL, TR-PL, XPS, TEM, and FTIR. The absorption and PL spectra were measured at each step of the patterning process to track any changes resulting from each individual step. The absorption and PL spectra showed nearly identical peak positions and full width at half-maximum (fwhm) values (Figure 2A,B). This consistency in the absorption and PL spectra suggests that there were no significant changes in the electronic band structure of QDs throughout the patterning process. This also implies that the patterning process was not

https://doi.org/10.1021/acsenergylett.3c01019
ACS Energy Lett. 2023, 8, 4210−4217

accompanied by core oxidation[30] or a significant decrease in shell thickness. Further corroborating this, the analysis of the P2p XPS spectra revealed that the variations in the oxidized indium phosphide ($InPO_x$) proportion were minimal (Figure S6, Table S1).

Furthermore, given that several studies have reported a crucial impact of acidic conditions on the PL characteristics of InP-based core/shell QDs (Figure S7),[31,32] we conducted high-resolution TEM studies to investigate the extent of Zn(Se,S) shell etching by the photogenerated chemicals (Figure S8). Even when a considerably higher amount of MBT (10 wt %) was used during sample fabrication compared to the standard patterning conditions (1−2 wt %), no significant differences were observed in the crystal structure and size distribution. This was in accordance with the observations in absorption and PL spectra, which showed negligible changes in peak positions and the fwhm upon patterning (Figure 2A,B). This observation was further supported by the results of grazing incidence small-angle X-ray scattering (GI-SAXS) measurements, which showed no significant changes in the QD size upon the patterning process (Figure S9). Consequently, we conclude that the patterning process with MBT did not result in a noticeable decrease in the shell thickness of the QDs.

Subsequently, we confirmed the absence of an MBT residue in the patterned InP-based QD film. To ensure the optimal optical and electrical properties of patterned InP-based QDs, it is crucial for the development process to effectively eliminate any remaining MBT from the patterned QD/MBT films. We conducted FTIR measurements to investigate the presence of the residual MBT. The FTIR spectra were measured with an excess amount (20 wt %) of MBT for each step of the patterning process (Figure 2C). The bands at 1600 cm^{-1} were identified as the stretching mode of the C═C bond between the benzene ring and triazine ring, whereas the 1550−1500 cm^{-1} bands were assigned to the C═C bond stretching in the benzene ring, both of which denote the characteristic peaks of MBT.[33] However, upon examination of the developed QD film, we did not observe any C═C stretching bands specific to MBT, indicating that there was almost no residual MBT present in the patterned QD films. Therefore, we can exclude the MBT residue from the possible origins of the PLQY reduction.

The occurrence of *in situ* ligand exchange from oleate ligands to chloride ligands was confirmed by observing the appearance of the Cl2p peak in the XPS spectra (Figure S10). Even though the amount of residual MBT was negligible after development, the Cl2p peak intensity of the developed InP QD film remained comparable to that of the QD/MBT film before development, indicating the presence of chloride ligands. However, the extent of *in situ* ligand exchange was found to be small; this was in accordance with the negligible changes in the QD size upon the patterning process as shown in TEM and GI-SAXS measurements (Figures S8 and S9). In addition, the FTIR peak intensities of zinc-bound oleates (at 1450 and 1490 cm^{-1}) were similar for the samples at the formulation, UV exposure, and development stages,[34] further supporting that the oleate ligands attached to the surface of the InP QDs were only marginally displaced during the patterning process (Figure 2C). This small degree of *in situ* ligand exchange is advantageous in preserving the PLQY of the QD films during patterning.

Based on the UV/vis, PL, XPS, TEM, and FTIR analyses, we were able to ascertain that the PLQY drop was not mainly caused by surface etching via photogenerated HCl, residual MBT, and core oxidation. Therefore, we conclude that the reduction in PLQY is primarily attributed to the generation of deep trap states through *in situ* ligand exchange. This conclusion is corroborated by a previous study, which suggests that substituting the organic ligands of InP/ZnS core/shell QDs with inorganic ligands (e.g., sulfur, chloride, etc.) can create hole trap states, leading to a significant increase in nonradiative recombination.[23] Such an increase in nonradiative recombination resulting from the generation of hole trap states can rationally explain the substantial alteration in the PLQY of InP-based QDs during the patterning process. Notably, the patterning process resulted in a ∼75% reduction in PLQY in comparison to the pristine InP-based QD film (Figure 2D).

However, in previous studies using CdSe-based QDs with the same Zn(Se,S) shell composition, such a pronounced PLQY drop was not observed. We suggest that this phenomenon may be attributed to the small electron potential barrier between the InP core and Zn(Se,S) shell, which induces a wider electron wave function distribution across the core and shell of the QDs compared to CdSe/Zn(Se,S) QDs.[35,36] To elucidate this, we investigated the changes in PL lifetime of InP/ZnSeS/ZnS and CdSe/ZnSeS/ZnS core/shell QD films with the addition of an electron quencher, 1,3,5-tris(*N*-phenylbenzimidazole-2-yl)benzene (TPBi), which is a commonly used electron-transporting material in QD LEDs. With the inclusion of TPBi, we observed a more pronounced decrease in the PL lifetime of InP-based QDs compared with CdSe-based QDs (Figure S11). Based on our observations, it can be inferred that InP/Zn(Se,S) QDs exhibit a wider distribution of electron wave function compared to CdSe/Zn(Se,S) QDs. This characteristic can make InP-based QDs more susceptible to the influence of deep trap states induced by exchanged chloride ligands. This proposition can be corroborated by comparing the effects of ligand exchange on the emissive characteristics of two different CdSe-based core/shell QDs: CdSe/CdS QDs[29] and CdSe/CdZnS QDs.[29] It is well-known that CdSe/CdS QDs have a smaller degree of electron confinement and a wider distribution of electron wave function than those of CdSe/CdZnS QDs.[37] The degree of increase in nonradiative recombination upon chloride ligand exchange was much larger in CdSe/CdS QDs than that in CdSe/CdZnS QDs;[22,29] these observations support our proposition on the vulnerability of InP QDs.

To suppress the nonradiative recombination caused by the deep trap states generated during the ink formulation and subsequent patterning process, we developed a "photoacid-generation rate control" method using an amine additive. We hypothesized that a small amount of amine can neutralize the HCl generated during the formulation and decrease photoacid-generation rate during UV exposure, thereby reducing the surface degradation caused by the protons and increasing the PLQY. In fact, a significant PLQY drop was observed at the QD/MBT ink formulation step (Figure 2D). We attributed this to the high photosensitivity of MBT, generating a small amount of HCl during dispersion in toluene (Figure S12). To neutralize the acidic characteristic of QD/MBT inks and control the acid-generation rate, we added a small amount of octylamine (0.1−0.5 vol %) during formulation. Consequently, the reduction in the PLQY during MBT formulation (before UV exposure) was substantially suppressed (Figure 3A).

https://doi.org/10.1021/acsenergylett.3c01019
ACS Energy Lett. 2023, 8, 4210−4217

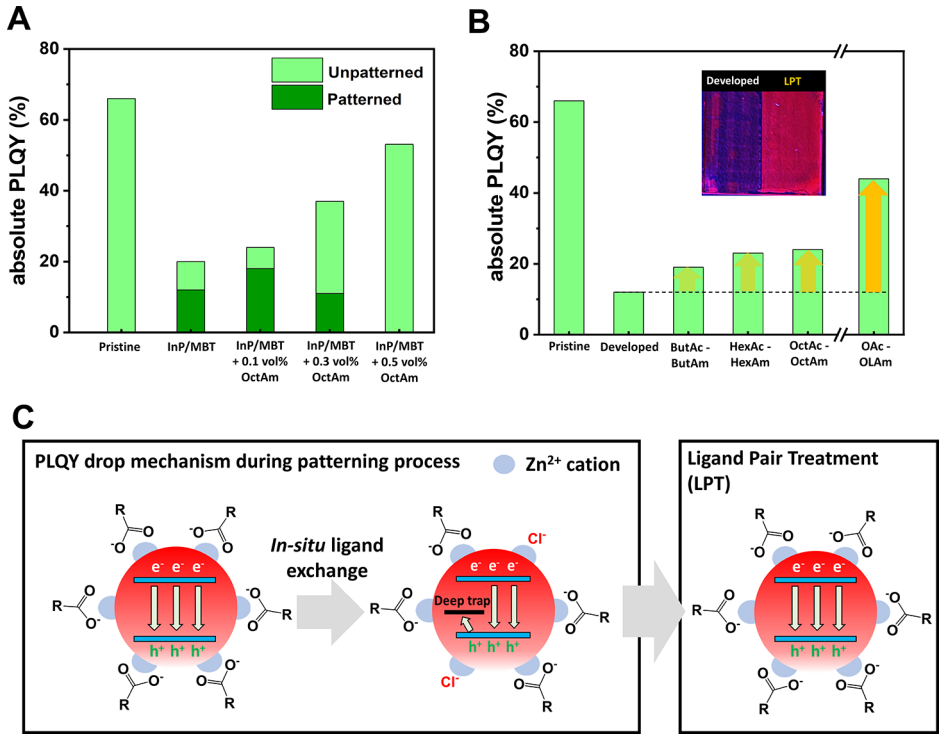

Figure 3. (A) PLQY change of InP-based core/shell QD films by incorporating octylamine (OctAm) additive with varying vol %. The legend "Unpatterned" refers to the PLQY at the formulation step, while "Patterned" refers to the final PLQY after the subsequent patterning steps (i.e., UV exposure and development) (dose: 100 mJ/cm^2 for InP/MBT and InP/MBT + 0.1 vol % octylamine, 200 mJ/cm^2 for InP/MBT + 0.3 vol % octylamine, and excess UV dose for InP/MBT + 0.5 vol % octylamine). (B) PLQY change of InP-based core/shell QD films caused by LPT with varying ligand chain length (dose: 100 mJ/cm^2 for all samples). MBT = 1.5 wt % for all samples in (A) and (B). (C) Schematic of PLQY drop and LPT mechanisms.

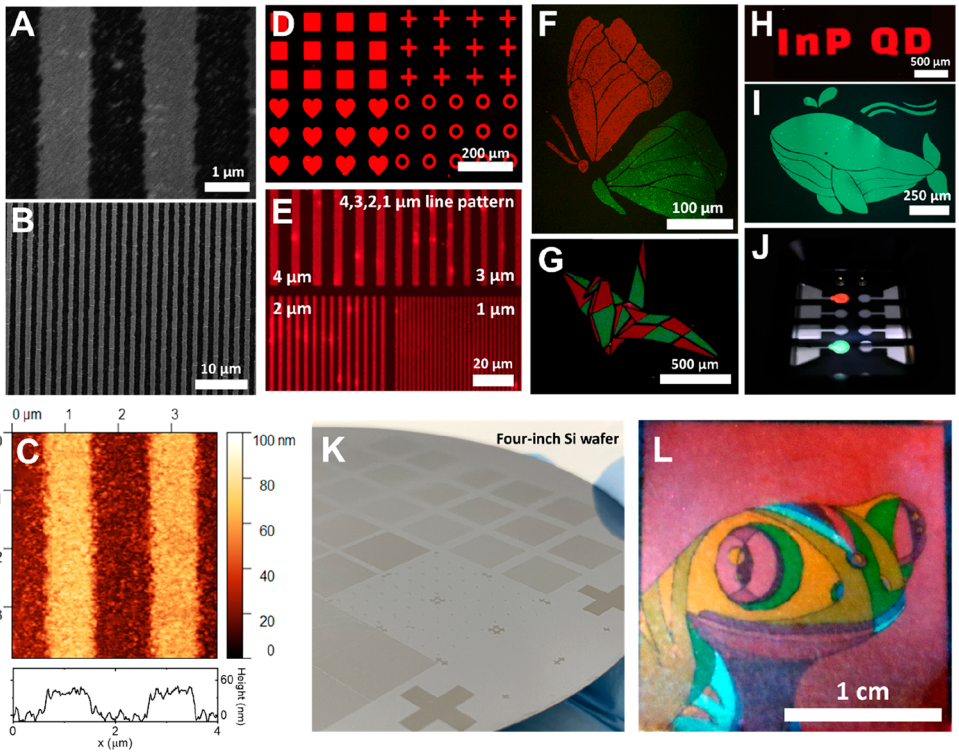

Figure 4. (A,B) SEM and (C) AFM images of 1 μm line patterns of InP-based QDs. (D–I) Fluorescence OM images of InP-based QD patterns: (D) various shapes, (E) 4, 3, 2, 1 μm line patterns, (F,G) red-green dual-color butterfly and crane patterns, (H) an InP QD word pattern, (I) a green whale pattern. (J) A photograph of operating patterned QD LEDs. (K) Direct optical lithography of QD at a 4 in. Si wafer. (L) An RGB frog pattern. The original image was created by Manuela Valencia Restrepo and used with permission.[38]

https://doi.org/10.1021/acsenergylett.3c01019
ACS Energy Lett. 2023, 8, 4210–4217

Furthermore, the addition of a small amount of octylamine (0.1 vol %) slightly suppressed the reduction in PLQY upon UV exposure by reducing the surface degradation by protons and achieving a minimal extent of *in situ* ligand exchange for patterning. However, an increase in the amount of octylamine to 0.3 vol % decreased the final PLQY of QD patterns. Furthermore, with 0.5 vol % octylamine, the QD patterns could not be achieved even with excess UV exposure. These effects after 0.1 vol % octylamine can be attributed to the competitive reaction of octylamine with HCl, decreasing the yield of the *in situ* ligand exchange reaction and thereby resulting in an increased UV dose (>500 mJ cm^{-2}) and photodegradation during patterning. Through these experimental results, we have confirmed that the minimization of both the UV dose and the exchange quantity of chloride ligands is crucial for securing patterns exhibiting a high PLQY.

To further increase the PLQY of the QD patterns, we introduced an LPT strategy for the patterned QD films. The detailed mechanism of LPT is described in the Supplementary text A in the Supporting Information. Despite following an optimized degree of *in situ* ligand exchange, the presence of chloride ligands generates deep trap states which decrease the PLQY of QD patterns. The application of the LPT strategy can exchange the chloride ligands on the surface of QDs with long-chain organic ligands while retaining pattern morphology and uniformity. The carboxylate ligands exchanged on the QD surface after LPT are expected to remove the deep trap states created by chloride ligands. To explore the relationship between the surface condition of InP-based QDs and PLQY more in detail, we applied various combinations of carboxylic acids and amines with different chain lengths to the LPT. In the case of core/shell QDs, it is well-known that ligands with short chains contribute more significantly to trap states.[24] Indeed, the extent of PLQY recovery was found to be dependent on the chain length of the ligands used in the process (Figure 3B), indicating a significant influence of the hole trap generation originating from surface ligands on the PLQY of QDs. Notably, the use of the oleic acid/oleylamine combination in LPT produced three times higher PLQY than patterned InP-based QDs (~67% compared to pristine InP QD film; Figure 3B). The effectiveness of LPT was further confirmed by XPS and TR-PL analyses. Even with an excess amount of MBT (6 wt %), the Cl 2p peak disappeared after LPT, confirming the respassivation of oleate ligands (Figure S13). Furthermore, the TR-PL results showed increases in the average PL lifetime and radiative recombination fraction upon LPT, also suggesting effective surface repassivation (Figure S14, Table S2). Additionally, we conducted AFM analysis to verify that LPT does not damage the patterns. The results confirmed that LPT is an ideal postprocessing technique as it does not affect the line width, LER, and pattern thickness of the patterns (Figures S15 and S16).

As shown in scanning electron microscope (SEM) and atomic force microscope (AFM) images, we were able to attain uniform and high-resolution patterns at a scale of 1 μm through the optimization of the MBT amount and UV dose (Figure 4A–C). Furthermore, we successfully achieved various shapes of patterns, including RG dual-color and RGB multicolor patterns (Figure 4D–L, Figure S17), demonstrating the feasibility of orthogonal processing in our method. Additionally, we demonstrated the capability of our direct optical lithography technique and LPT process to fabricate patterned QD LED pixels (Figure 4J, Figure S18). Notably, we observed that the decreased device efficiency upon patterning improved with the LPT process (Figure S18D; see Supporting Information in text B and C for more discussion). This method is also scalable; the patterning process was able to be successfully performed even on large-scale 4 in. wafers with CdSe-based and InP-based QDs (Figure 4K, Figure S19). These results illustrate the versatility and potential of the proposed approach for practical optoelectronics applications.

In conclusion, we developed an advanced direct optical lithography method to fabricate high-resolution patterns of InP-based core–shell QDs while minimizing the degradation of their luminescence characteristics. By using a trichloro triazine-based PAG, we achieved 1 μm scale QD patterns with uniform surface morphology, orthogonal RGB patterns, and patterned QD LEDs. To mitigate the degradation of QDs, we devised an effective solid-state ligand exchange strategy, called "Ligand Pair Treatment (LPT)", where the *in situ* exchanged chloride ligands are re-exchanged with amine/carboxylate pair-ligands. The use of LPT significantly recovered the PLQY of QD patterns, up to nearly 70% of the pristine QD film without variations in their structural properties. Furthermore, we investigated the possible origins of significant PLQY drop upon patterning and revealed that the primary origin was the generation of deep trap states by the chloride ligands during the *in situ* ligand exchange process; these deep trap states increase the proportion of nonradiative recombination. To the best of our knowledge, this study is the first identification and elucidation of the underlying origins for the PLQY reduction during the patterning process of InP-based core/shell QDs. These results highlight the great potential of our method for various optoelectronics and display applications and present a big step toward the industrialization of direct optical lithography.

■ ASSOCIATED CONTENT

Supporting Information

The Supporting Information is available free of charge at https://pubs.acs.org/doi/10.1021/acsenergylett.3c01019.

Materials and experimental methods for the QD synthesis, patterning, and characterization; Text SA–C, mechanism of LPT, comparison of device characteristics, and discussion on the impact of the LPT process on QLED characteristics; Figures S1–S19, schematic of the patterning process, TEM images of QDs, absorption and PL spectra, OM and AFM images of QD patterns, XPS spectra, GI-SAXS spectra, TR-PL curves, a photograph of 4-in.-wafer-scale patterns, EL characteristics; Tables S1 and S2, proportion of integrated area and fitting parameter summary of TR-PL curves (PDF)

■ AUTHOR INFORMATION

Corresponding Authors

Dmitri V. Talapin − *Department of Chemistry, James Franck Institute, and Pritzker School of Molecular Engineering, University of Chicago, Chicago, Illinois 60637, United States; Center for Nanoscale Materials, Argonne National Laboratory, Argonne, Illinois 60439, United States;* orcid.org/0000-0002-6414-8587; Email: dvtalapin@uchicago.edu

Himchan Cho − *Department of Materials Science and Engineering, Graduate School of Semiconductor Technology, Korea Advanced Institute of Science and Technology, Daejeon*

https://doi.org/10.1021/acsenergylett.3c01019
ACS Energy Lett. 2023, 8, 4210–4217

34141, Republic of Korea; orcid.org/0000-0001-6372-5787; Email: himchan@kaist.ac.kr

Authors

Jaehwan Lee − *Department of Materials Science and Engineering, Korea Advanced Institute of Science and Technology, Daejeon 34141, Republic of Korea*

Jaeyeong Ha − *Department of Materials Science and Engineering, Korea Advanced Institute of Science and Technology, Daejeon 34141, Republic of Korea*

Hyungdoh Lee − *Department of Materials Science and Engineering, Korea Advanced Institute of Science and Technology, Daejeon 34141, Republic of Korea*

Hyunjin Cho − *Department of Chemical and Biomolecular Engineering, Korea Advanced Institute of Science and Technology, Daejeon 34141, Republic of Korea*

Doh C. Lee − *Department of Chemical and Biomolecular Engineering, Korea Advanced Institute of Science and Technology, Daejeon 34141, Republic of Korea;* orcid.org/0000-0002-3489-6189

Complete contact information is available at: https://pubs.acs.org/10.1021/acsenergylett.3c01019

Notes

The authors declare no competing financial interest.

■ ACKNOWLEDGMENTS

This work was supported by the National Research Foundation of Korea (NRF) grant funded by the Ministry of Science and ICT, Korea (NRF-2022M3H4A1A03085346). This research has been supported by the Technological Innovation R&D Program (S3207641) funded by the Ministry of SMEs and Startups (MSS, Korea). This work was supported by Samsung Advanced Institute of Technology (IO220810-01911-01). This work was supported by KAIST under KAIST International Joint Research Support Program (N11230002). D.V.T. acknowledges support by Samsung QD Cluster Collaboration, by NSF under award number CHE-1905290, and by the Center for Hierarchical Materials Design (CHiMad) supported by U.S. Department of Commerce, National Institute of Standards and Technology under financial assistance award number 70NANB14H012.

■ REFERENCES

(1) Dai, X.; Zhang, Z.; Jin, Y.; Niu, Y.; Cao, H.; Liang, X.; Chen, L.; Wang, J.; Peng, X. Solution-Processed, High-Performance Light-Emitting Diodes Based on Quantum Dots. *Nature* **2014**, *515* (7525), 96−99.

(2) Kagan, C. R.; Lifshitz, E.; Sargent, E. H.; Talapin, D. V. Building Devices from Colloidal Quantum Dots. *Science* **2016**, *353* (6302), 885−894.

(3) Talapin, D. V.; Lee, J. S.; Kovalenko, M. V.; Shevchenko, E. V. Prospects of Colloidal Nanocrystals for Electronic and Optoelectronic Applications. *Chem. Rev.* **2010**, *110* (1), 389−458.

(4) Won, Y. H.; Cho, O.; Kim, T.; Chung, D. Y.; Kim, T.; Chung, H.; Jang, H.; Lee, J.; Kim, D.; Jang, E. Highly Efficient and Stable InP/ZnSe/ZnS Quantum Dot Light-Emitting Diodes. *Nature* **2019**, *575* (7784), 634−638.

(5) Srivastava, A. K.; Zhang, W.; Schneider, J.; Halpert, J. E.; Rogach, A. L. Luminescent Down-Conversion Semiconductor Quantum Dots and Aligned Quantum Rods for Liquid Crystal Displays. *Adv. Sci.* **2019**, *6*, No. 1901345.

(6) Kim, K.; Yoo, D.; Choi, H.; Tamang, S.; Ko, J. H.; Kim, S.; Kim, Y. H.; Jeong, S. Halide-Amine Co-Passivated Indium Phosphide Colloidal Quantum Dots in Tetrahedral Shape. *Angew. Chemie - Int. Ed.* **2016**, *55* (11), 3714−3718.

(7) Ramasamy, P.; Ko, K. J.; Kang, J. W.; Lee, J. S. Two-Step "Seed-Mediated" Synthetic Approach to Colloidal Indium Phosphide Quantum Dots with High-Purity Photo- and Electroluminescence. *Chem. Mater.* **2018**, *30* (11), 3643−3647.

(8) Kwon, Y.; Oh, J.; Lee, E.; Lee, S. H.; Agnes, A.; Bang, G.; Kim, J.; Kim, D.; Kim, S. Evolution from Unimolecular to Colloidal-Quantum-Dot-like Character in Chlorine or Zinc Incorporated InP Magic Size Clusters. *Nat. Commun.* **2020**, *11*, 3127.

(9) Park, S. J.; Keum, C.; Zhou, H.; Lee, T. W.; Choe, W.; Cho, H. Progress and Prospects of Nanoscale Emitter Technology for AR/VR Displays. *Adv. Mater. Technol.* **2022**, No. 2201070.

(10) Wang, Y.; Fedin, I.; Zhang, H.; Talapin, D. V. Direct Optical Lithography of Functional Inorganic Nanomaterials. *Science* **2017**, *357* (6349), 385−388.

(11) Cho, H.; Pan, J. A.; Wu, H.; Lan, X.; Coropceanu, I.; Wang, Y.; Cho, W.; Hill, E. A.; Anderson, J. S.; Talapin, D. V. Direct Optical Patterning of Quantum Dot Light-Emitting Diodes via In Situ Ligand Exchange. *Adv. Mater.* **2020**, *32*, No. 2003805.

(12) Fu, Z.; Zhou, L.; Yin, Y.; Weng, K.; Li, F.; Lu, S.; Liu, D.; Liu, W.; Wu, L.; Yang, Y.; Li, H.; Duan, L.; Xiao, H.; Zhang, H.; Li, J. Direct Photo-Patterning of Efficient and Stable Quantum Dot Light-Emitting Diodes via Light-Triggered, Carbocation-Enabled Ligand Stripping. *Nano Lett.* **2023**, *23* (5), 2000−2008.

(13) Pan, J. A.; Ondry, J. C.; Talapin, D. V. Direct Optical Lithography of CsPbX3Nanocrystals via Photoinduced Ligand Cleavage with Postpatterning Chemical Modification and Electronic Coupling. *Nano Lett.* **2021**, *21* (18), 7609−7616.

(14) Wang, Y.; Shan, X.; Tang, Y.; Liu, T.; Li, B.; Jin, P.; Liang, K.; Li, D.; Yang, Y. M.; Shen, H.; Zhu, B.; Ji, B. Direct Optical Patterning of Nanocrystal-Based Thin-Film Transistors and Light-Emitting Diodes through Native Ligand Cleavage. *ACS Appl. Nano Mater.* **2022**, *5* (6), 8457−8466.

(15) Liu, D.; Weng, K.; Lu, S.; Li, F.; Abudukeremu, H.; Zhang, L.; Yang, Y.; Hou, J.; Qiu, H.; Fu, Z.; Luo, X.; Duan, L.; Zhang, Y.; Zhang, H.; Li, J. Direct Optical Patterning of Perovskite Nanocrystals with Ligand Cross-Linkers. *Sci. Adv.* **2022**, *8*, No. eabm8433.

(16) Hahm, D.; Lim, J.; Kim, H.; Shin, J. W.; Hwang, S.; Rhee, S.; Chang, J. H.; Yang, J.; Lim, C. H.; Jo, H.; Choi, B.; Cho, N. S.; Park, Y. S.; Lee, D. C.; Hwang, E.; Chung, S.; Kang, C. mo; Kang, M. S.; Bae, W. K. Direct Patterning of Colloidal Quantum Dots with Adaptable Dual-Ligand Surface. *Nat. Nanotechnol.* **2022**, *17* (9), 952−958.

(17) Ko, J.; Chang, J. H.; Jeong, B. G.; Kim, H. J.; Joung, J. F.; Park, S.; Choi, D. H.; Bae, W. K.; Bang, J. Direct Photolithographic Patterning of Colloidal Quantum Dots Enabled by UV-Crosslinkable and Hole-Transporting Polymer Ligands. *ACS Appl. Mater. Interfaces* **2020**, *12* (37), 42153−42160.

(18) Jun, S.; Jang, E.; Park, J.; Kim, J. Photopatterned Semiconductor Nanocrystals and Their Electroluminescence from Hybrid Light-Emitting Devices. *Langmuir* **2006**, *22* (6), 2407−2410.

(19) Park, J. J.; Prabhakaran, P.; Jang, K. K.; Lee, Y.; Lee, J.; Lee, K.; Hur, J.; Kim, J. M.; Cho, N.; Son, Y.; Yang, D. Y.; Lee, K. S. Photopatternable Quantum Dots Forming Quasi-Ordered Arrays. *Nano Lett.* **2010**, *10* (7), 2310−2317.

(20) Xiao, P.; Zhang, Z.; Ge, J.; Deng, Y.; Chen, X.; Zhang, J. R.; Deng, Z.; Kambe, Y.; Talapin, D. V.; Wang, Y. Surface Passivation of Intensely Luminescent All-Inorganic Nanocrystals and Their Direct Optical Patterning. *Nat. Commun.* **2023**, *14* (1), 49−59.

(21) Gao, H.; Qie, Y.; Zhao, H.; Li, F.; Guo, T.; Hu, H. High-Performance, High-Resolution Quantum Dot Light-Emitting Devices through Photolithographic Patterning. *Org. Electron.* **2022**, *108*, No. 106609.

(22) Baronnier, J.; Mahler, B.; Boisron, O.; Dujardin, C.; Kulzer, F.; Houel, J. Optical Properties of Fully Inorganic Core/Gradient-Shell CdSe/CdZnS Nanocrystals at the Ensemble and Single-Nanocrystal Levels. *Phys. Chem. Chem. Phys.* **2021**, *23* (39), 22750−22759.

(23) Yu, S.; Fan, X. B.; Wang, X.; Li, J.; Zhang, Q.; Xia, A.; Wei, S.; Wu, L. Z.; Zhou, Y.; Patzke, G. R. Efficient Photocatalytic Hydrogen Evolution with Ligand Engineered All-Inorganic InP and InP/ZnS Colloidal Quantum Dots. *Nat. Commun.* **2018**, *9*, 4009.
(24) Zeng, S.; Li, Z.; Tan, W.; Si, J.; Huang, Z.; Hou, X. Ultrafast Electron Transfer Dynamics Affected by Ligand Chain Length in InP/ZnS Core/Shell Quantum Dots. *J. Phys. Chem. C* **2022**, *126* (21), 9091−9098.
(25) Wang, Y.; Pan, J. A.; Wu, H.; Talapin, D. V. Direct Wavelength-Selective Optical and Electron-Beam Lithography of Functional Inorganic Nanomaterials. *ACS Nano* **2019**, *13* (12), 13917−13931.
(26) Kim, J.; Kwon, S. M.; Kang, Y. K.; Kim, Y. H.; Lee, M. J.; Han, K.; Facchetti, A.; Kim, M. G.; Park, S. K. A Skin-like Two-Dimensionally Pixelized Full-Color Quantum Dot Photodetector. *Sci. Adv.* **2019**, *5*, No. eaax8801.
(27) Li, L.; Chakrabarty, S.; Spyrou, K.; Ober, C. K.; Giannelis, E. P. Studying the Mechanism of Hybrid Nanoparticle Photoresists: Effect of Particle Size on Photopatterning. *Chem. Mater.* **2015**, *27* (14), 5027−5031.
(28) Liu, S. F.; Hou, Z. W.; Lin, L.; Li, F.; Zhao, Y.; Li, X. Z.; Zhang, H.; Fang, H. H.; Li, Z.; Sun, H. B. 3D Nanoprinting of Semiconductor Quantum Dots by Photoexcitation-Induced Chemical Bonding. *Science* **2022**, *377* (6610), 1112−1116.
(29) Sayevich, V.; Guhrenz, C.; Sin, M.; Dzhagan, V. M.; Weiz, A.; Kasemann, D.; Brunner, E.; Ruck, M.; Zahn, D. R. T.; Leo, K.; Gaponik, N.; Eychmüller, A. Chloride and Indium-Chloride-Complex Inorganic Ligands for Efficient Stabilization of Nanocrystals in Solution and Doping of Nanocrystal Solids. *Adv. Funct. Mater.* **2016**, *26* (13), 2163−2175.
(30) Chen, P. R.; Lai, K. Y.; Chen, H. S. Roles of Alcohols and Existing Metal Ions in Surface Chemistry and Photoluminescence of InP Cores. *Mater. Adv.* **2021**, *2* (18), 6039−6048.
(31) Litvinov, I. K.; Belyaeva, T. N.; Salova, A. V.; Aksenov, N. D.; Leontieva, E. A.; Orlova, A. O.; Kornilova, E. S. Quantum Dots Based on Indium Phosphide (InP): The Effect of Chemical Modifications of the Organic Shell on Interaction with Cultured Cells of Various Origins. *Cell tissue biol.* **2018**, *12* (2), 135−145.
(32) Litvinov, I.; Salova, A.; Aksenov, N.; Kornilova, E.; Belyaeva, T. Microenvironmental Impact on InP/ZnS-Based Quantum Dots in In Vitro Models and in Living Cells: Spectrally- and Time-Resolved Luminescence Analysis. *Int. J. Mol. Sci.* **2023**, *24* (3), 2699−2716.
(33) Li, L.; Zhu, D.; Peng, X.; Xiao, P. Visible-Light-Sensitive Polymerizable and Polymeric Triazine-Based Photoinitiators with Enhanced Migration Stability. *Catalysts* **2022**, *12* (11), 1305−1316.
(34) Anderson, N. C.; Hendricks, M. P.; Choi, J. J.; Owen, J. S. Ligand Exchange and the Stoichiometry of Metal Chalcogenide Nanocrystals: Spectroscopic Observation of Facile Metal-Carboxylate Displacement and Binding. *J. Am. Chem. Soc.* **2013**, *135* (49), 18536−18548.
(35) Jang, D.; Han, Y.; Baek, S.; Kim, J. Theoretical Comparison of the Energies and Wave Functions of the Electron and Hole States between CdSe- and InP-Based Core/Shell/Shell Quantum Dots: Effect of the Bandgap Energy of the Core Material on the Emission Spectrum. *Opt. Mater. Express* **2019**, *9* (3), 1257−1270.
(36) Jang, E.; Kim, Y.; Won, Y. H.; Jang, H.; Choi, S. M. Environmentally Friendly InP-Based Quantum Dots for Efficient Wide Color Gamut Displays. *ACS Energy Lett.* **2020**, *5* (4), 1316−1327.
(37) Talapin, D. V.; Mekis, I.; Gotzinger, S.; Kornowski, A.; Benson, O.; Weller, H. CdSe/CdS/ZnS and CdSe/ZnSe/ZnS Core - Shell - Shell Nanocrystals. *J. Phys. Chem. B* **2004**, *108*, 18826−18831.
(38) "RGB frog image #Carnimals by Manueal V. Restroepo" (2023, July 6) URL: https://www.behance.net/gallery/68452005/Carnimals.

https://doi.org/10.1021/acsenergylett.3c01019
ACS Energy Lett. 2023, 8, 4210−4217